arXiv:astro-ph/0112567v1 31 Dec 2001

First *XMM-Newton* observations of strongly magnetic cataclysmic variables - II. Timing studies of DP Leo and WW Hor

Dirk Pandel[1], France A. Cordova[1], Robert E. Shirey[1], Gavin Ramsay[2], Mark Cropper[2], Keith O. Mason[2], Rudi Much[3], Dave Kilkenny[4]
[1] *Department of Physics, University of California, Santa Barbara, CA 93106, USA*
[2] *Mullard Space Science Lab, University College London, Holmbury St. Mary, Dorking, Surrey, RH5 6NT, UK*
[3] *Astrophysics Division, ESTEC, 2200, AG Noordwijk, The Netherlands*
[4] *South African Astronomical Observatory, PO Box 9, Observatory 7935, South Africa*

1 February 2008

ABSTRACT

XMM-Newton was used to observe two eclipsing, magnetic cataclysmic variables, DP Leo and WW Hor, continuously for three orbital cycles each. Both systems were in an intermediate state of accretion. For WW Hor we also obtained optical light curves with the *XMM-Newton* Optical Monitor and from ground-based observations. Our analysis of the X-ray and optical light curves allows us to constrain physical and geometrical parameters of the accretion regions and derive orbital parameters and eclipse ephemerides of the systems. For WW Hor we directly measure horizontal and vertical temperature variations in the accretion column. From comparisons with previous observations we find that changes in the accretion spot longitude are correlated with the accretion rate. For DP Leo the shape of the hard X-ray light curve is not as expected for optically thin emission, showing the importance of optical depth effects in the post-shock region. We find that the spin period of the white dwarf is slightly shorter than the orbital period and that the orbital period is decreasing faster than expected for energy loss by gravitational radiation alone.

Key words: Stars: binaries: eclipsing – Stars: magnetic field – Stars: novae, cataclysmic variables – Stars: individual: DP Leo, WW Hor – X-rays: stars

1 INTRODUCTION

DP Leo and WW Hor are two eclipsing binary systems of type AM Her, a class of magnetic cataclysmic variables also referred to as polars because of their strongly polarized optical emission. In these systems the strong magnetic field of the white dwarf primary causes it to rotate synchronously with the orbital motion of the binary. Due to the strong magnetic field, the accretion stream from the Roche lobe filling secondary does not form a disk, but rather follows the magnetic field lines onto the white dwarf's surface. Slightly above the photosphere the accretion flow forms a shock that heats the gas to temperatures above $\sim 10^8$K. The gas below the shock front then cools and settles onto the photosphere (Wu 2000). Models of the accretion region suggest three major spectral components. Thermal bremsstrahlung is emitted in the X-ray band by the hot gas between the shock front and the surface. The photosphere below the shock is heated to temperatures of $\sim 10^5$K by reprocessing of bremsstrahlung photons and by dense filaments in the accretion stream (Kuijpers & Pringle 1982), giving rise to a blackbody component that extends from the UV to the soft X-ray band. The strong magnetic field at the surface of the white dwarf causes the shock-heated electrons to emit strongly polarized cyclotron radiation in the optical and IR bands. A comprehensive review of polars is given in Cropper (1990).

Much has been learned about the accretion region in polars from optical polarimetry. These observations, however, are only able to reveal the physical conditions that give rise to the cyclotron radiation. To fully understand the structure of the post-shock region and to test dynamical models of the accretion flow, the thermal bremsstrahlung and the blackbody component, both visible in the X-ray band, need to be studied as well. Past X-ray observations were limited by low sensitivity and a narrow X-ray bandpass. With the high sensitivity of *XMM-Newton* and its coverage of the 0.1–12 keV band we can now obtain light curves and spectra with unprecedented quality. This will allow us to indepen-

© 2002 RAS

Table 1. Details of the observations (see also Section 2.1)

Object	Instrument	Beginning of Observation (UTC)		Duration	Filter	Instrument mode	Timing resolution	Aperture radius	Event pattern
DP Leo	EPIC MOS 1	22 Nov 2000	4:55:02	22340 s	Thin 1	full window	2.6 s	25”	0–12
	EPIC MOS 2	”	4:54:54	22348 s	Thin 1	full window	2.6 s	25”	0–12
	EPIC PN	”	5:36:22	20034 s	Thin 1	full window	0.073 s	18”	0–12
WW Hor	EPIC MOS 1	4 Dec 2000	3:37:25	23543 s	Thin 1	full window	2.6 s	25”	0–12
	EPIC MOS 2	”	3:37:20	23548 s	Thin 1	full window	2.6 s	25”	0–12
	EPIC PN	”	4:18:48	21149 s	Thin 1	full window	0.073 s	18”	0–12
	Optical Monitor	”	3:30:09	9 × 2200 s	B	fast timing	0.5 s	3.2”	—
	SAAO (1.0 m)	2 Dec 2000	19:41:35	7140 s	R	—	60 s	—	—

dently study the bremsstrahlung and the blackbody component and derive the physical and geometrical properties of the accretion regions.

In this paper we analyze X-ray and optical light curves of two polars in order to constrain the geometry of the accretion regions, investigate properties of the X-ray emitting gas, determine parameters of the binary systems, and find changes in the accretion longitudes and orbital periods. We present a detailed spectral analysis of these data in Ramsay et al. (2001).

DP Leo, originally named E1114+182, was the first known eclipsing polar. This binary system, which has an orbital period of 89.8 min, was discovered serendipitously with the *Einstein* observatory and quickly identified as a polar because of its strongly modulated, polarized emission (Biermann et al. 1985). Robinson & Cordova (1994) and Bailey et al. (1993) later found that the accretion spot longitude is changing by ∼2° per year, suggesting a slightly asynchronous rotation of the white dwarf. We have shown in Ramsay et al. (2001) that the X-ray spectrum obtained with *XMM-Newton* contains in addition to the soft blackbody component a previously undetected hard bremsstrahlung component. Using the X-ray spectrum we derived a white dwarf mass of $\sim 1.4\ M_\odot$.

WW Hor (EXO 023432-5232), which has an orbital period of 115.5 min, was discovered as a serendipitous X-ray source with *EXOSAT* and later identified as a polar (Beuermann et al. 1987). Some of the system parameters were derived by Bailey et al. (1988), but orbital inclination and accretion spot latitude could not be determined. A significant change of the accretion longitude over time was found by Bailey et al. (1993). As we have shown in Ramsay et al. (2001), the *XMM-Newton* spectrum does not contain the blackbody component typically found in polars at soft X-ray energies. From the X-ray spectrum we derived a white dwarf mass of $\sim 1.1\ M_\odot$.

2 OBSERVATIONS AND ANALYSIS

2.1 Observations and data reduction

DP Leo and WW Hor were observed with *XMM-Newton* for more than 20 ks each, providing us with continuous X-ray data from all three EPIC instruments. We did not use the data from the RGS instruments due to their low signal-to-noise ratio. WW Hor was also observed with the *XMM-Newton* Optical Monitor and from the ground with the SAAO 1.0-m telescope. Details of the observations are shown in Table 1.

X-ray light curves were extracted using circular apertures with the radii shown in Table 1. For the background extraction we used regions near the source image and on the same CCD. In the DP Leo data we found several periods with an increased background rate, each lasting ∼1 ks. The largest increase occurred at the end of the observation so that we excluded the last 2 ks. No significant fluctuations of the background rate were found in the WW Hor data. After the initial data reduction we had for each target continuous X-ray data covering three complete orbital cycles available for our analysis.

During the WW Hor observation the *XMM-Newton* Optical Monitor was operating in fast timing mode with a time resolution of 0.5 s. The Optical Monitor performed 9 consecutive B-band observations with a duration of 2200 s each and separated by 300 s. The location of the source image on the detector coincided with the edge of the central stray light ring (Mason et al. 2001). This introduced uncertainties into the background calculation.

2.2 Light curve analysis

For our analysis we combined the EPIC MOS and PN data by adding the identically binned and background subtracted light curves from the three X-ray instruments. We did not observe differences between the individual MOS and PN light curves beyond those expected from statistical fluctuations. Because of the still uncertain calibration of the encircled energy fraction we did not apply a correction for the aperture sizes and the count rates quoted throughout the paper reflect only photons detected inside these apertures. The combined MOS and PN light curves over the 0.1–12 keV band are shown in Fig. 1. In order to improve the signal-to-noise ratio for our analysis and to reduce the fluctuations due to flaring we folded the light curves on the known orbital periods (5388 s for DP Leo (Robinson & Cordova 1994) and 6929 s for WW Hor (Beuermann et al. 1990)). The centre of the eclipse was chosen as orbital phase zero. Folded X-ray light curves are shown in Fig. 2a–c and 4a–c.

The eclipse ingress and egress durations for both objects are very short, near the limit of resolvability of the X-ray instruments (Fig. 3 and 5). We used a maximum likelihood method and the simple model of a circular, flat, homogeneous, face-on emission region to fit the eclipse profiles. Ingress and egress durations quoted throughout the paper

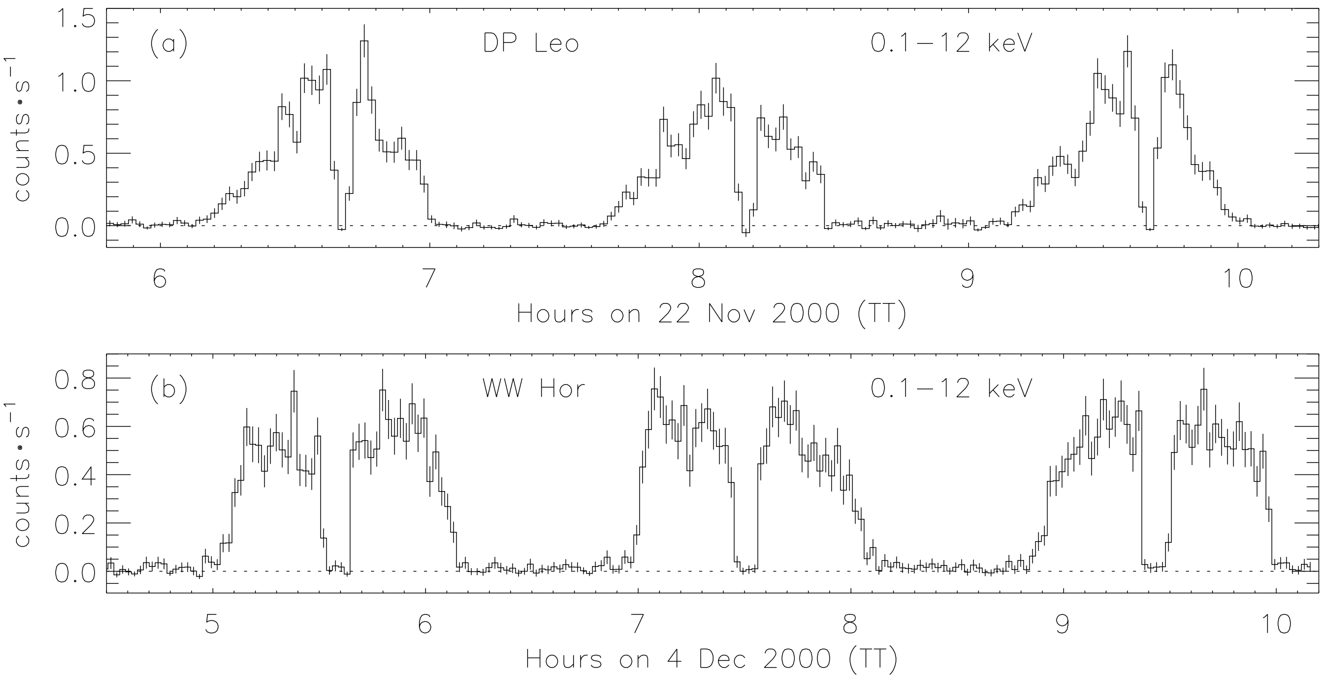

Figure 1. X-ray light curves for DP Leo and WW Hor obtained with *XMM-Newton*. Figures show the combined EPIC MOS and PN count rates over three orbital cycles in the 0.1–12 keV energy range. The light curves can be clearly separated into bright and faint phases each lasting about half of the orbit. During the faint phase the accretion region is on the hemisphere of the white dwarf facing away from us. The narrow dip during the bright phase is the eclipse of the white dwarf by the secondary star.

measure the diameter of this disk-like region. The width and centre of an eclipse were determined from the two points where the flux is half of its average value immediately before or after the eclipse. Photon arrival times were corrected to the solar system barycentre and the times of eclipse in this paper are shown as Barycentric Julian Dates (BJD) in Terrestrial Time (TT). The eclipse centres in Tables 2 and 3 refer to the first eclipses in Fig. 1. It should be noted that the time system used for *XMM-Newton* data is TT and not UTC as stated in the documentation of the Science Analysis System (XMM Helpdesk, priv. comm.). Due to this incorrect information Schwope et al. (2002), using the *XMM-Newton* data for DP Leo, overestimated the time of eclipse by ∼64 s.

2.3 DP Leo

As discussed in Ramsay et al. (2001), the X-ray spectrum of DP Leo shows two distinct components, a soft blackbody component dominating the flux below 0.3 keV and a previously undetected hard bremsstrahlung component dominating above this energy. The total flux observed with *XMM-Newton* is dominated by the soft blackbody component with more than 70 per cent of the X-rays in the energy range 0.1–0.3 keV. Folded light curves for various energy ranges are shown in Fig. 2. By choosing 0.3 keV as the upper limit for the soft band we almost completely separated the soft blackbody and the hard bremsstrahlung component with only a few per cent contamination remaining.

Surprisingly the light curves representing the bremsstrahlung component (Fig. 2b,c) do not show the top-hat shape that is expected for an optically thin post-shock region. Instead they appear to follow a cosine profile during the bright phase, which is consistent with optically thick emission (see Section 3.1.5 for further discussion). To the 0.3–12 keV light curve we fitted a cosine function with variable width and peak position (solid curves in Fig. 2b,c). We obtained a good fit ($\chi^2_{red} = 1.1$) with a bright phase duration of 0.57(1) and a centre at phase $-0.070(3)$. The latter value corresponds to an accretion spot longitude of $25^\circ \pm 1^\circ$. Here a longitude of 0° is defined by the line between the two stars and the positive sign indicates that the accretion spot is ahead of the secondary.

The light curve of the soft blackbody component (Fig. 2a) has a complex and asymmetric structure not visible in the harder X-ray bands (Fig. 2b,c). The asymmetry can also be seen in the hardness ratio (Fig. 2e) which shows a softening of the spectrum throughout the bright phase. Fig. 1a shows that some of this complex structure is due to short, random flares. It appears that the flares are concentrated around the eclipse and do not occur at the beginning of the bright phase. We discuss the shape of the soft X-ray light curve further in Section 3.1.6.

Folded X-ray light curves near the eclipse are shown in Fig. 3. The rapid decline to and rise from the eclipse is not resolved, except for the ingress in the 0.1–0.3 keV band which lasted 40 ± 10 s. We find an upper limit of 11 s for the egress duration in the 0.1–0.3 keV band and 40 s for the ingress and egress durations in the 0.3–12 keV band. This is consistent with the result by Stockman et al. (1994) who measured an ingress/egress duration of ∼8 s in the optical and UV. A possible explanation for the difference between ingress and egress in the 0.1–0.3 keV band is discussed in Section 3.1.6.

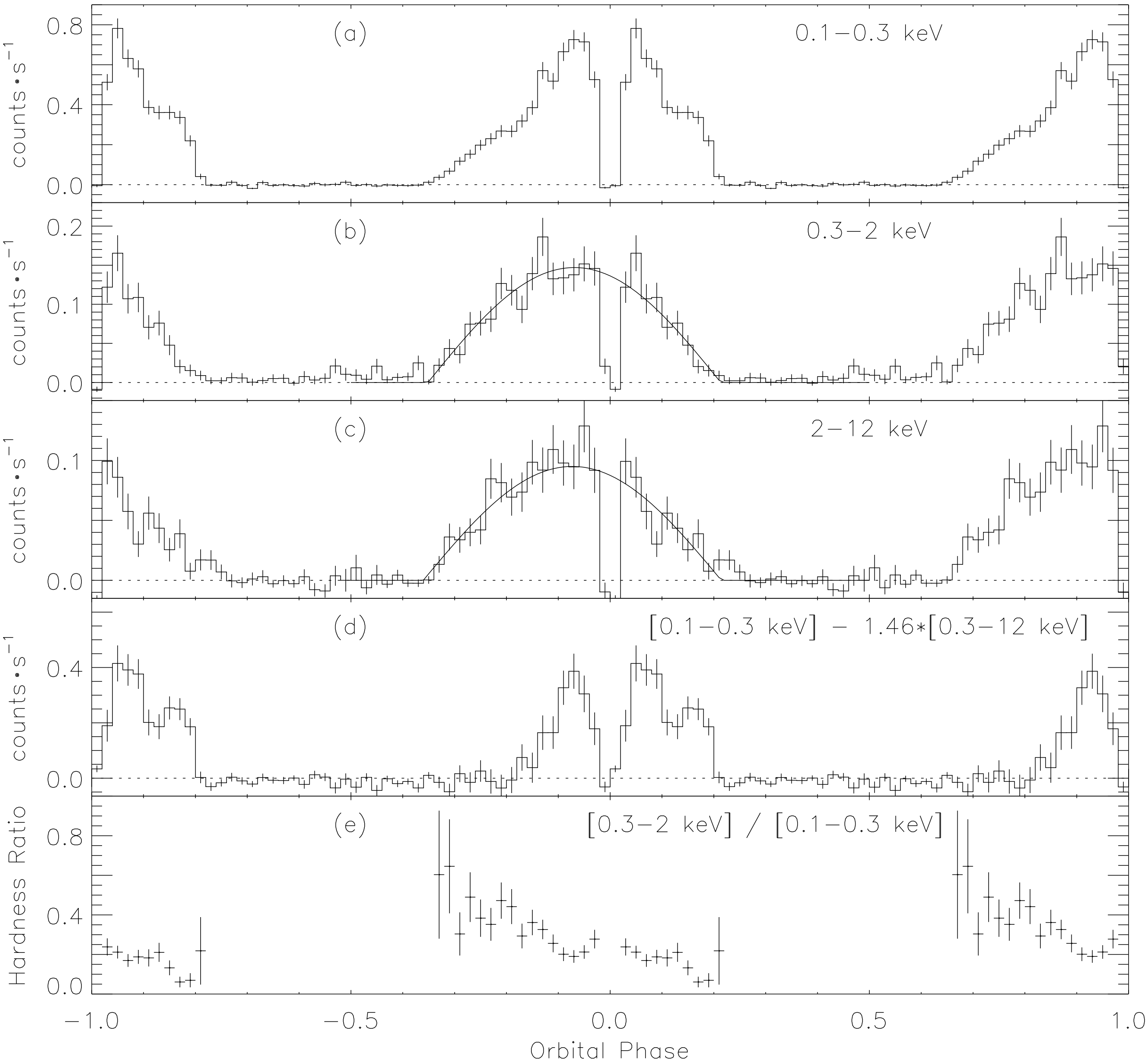

Figure 2. X-ray light curves for DP Leo folded on the orbital period of 5388 s (89.8 min). *(a)* Soft blackbody component. *(b,c)* Hard bremsstrahlung component; Solid curve is a cosine fitted with variable width and centre. *(d)* Residual of light curve (a) after the cosine profile shown in (b,c) has been subtracted (see Section 3.1.6). *(e)* Hardness ratio; Points with large uncertainties have been omitted.

2.4 WW Hor

The folded X-ray light curves for WW Hor (Fig. 4a–c) roughly exhibit a top-hat shape. This is expected for an optically thin emission region, since the observed flux does not change with the viewing angle unless part of the region becomes obscured by one of the stars. In Fig. 4a–c the transitions between bright and faint phases are slower for the 0.1–0.7 keV band, indicating that the soft X-rays originate from a larger region than the hard X-rays. This can also be seen in the hardness ratio (Fig. 4f) which shows that the spectrum is softer near phase ±0.30, when the hard X-ray emitting inner region of the accretion spot is not visible, and is harder near phase ±0.25, when only the soft X-ray emitting outer region is partially obscured. The slower rise and decline in the soft X-ray light curve might also be due to a non-negligible optical depth in the post-shock region. It is generally thought that optical depth effects are not important for bremsstrahlung, but Cropper et al. (2000) argue that electron scattering might produce a harder X-ray spectrum when the accretion column is viewed from the side. However, Fig. 4f clearly shows a softer spectrum at the beginning and end of the bright phase.

In the light curves we determined the duration of the rise and decline near phase ±0.25, and the width and centre of the bright phase by fitting the profile expected for an optically thin, circular and flat emission region. Results are shown in Table 3. As discussed in Section 3.2.5 these

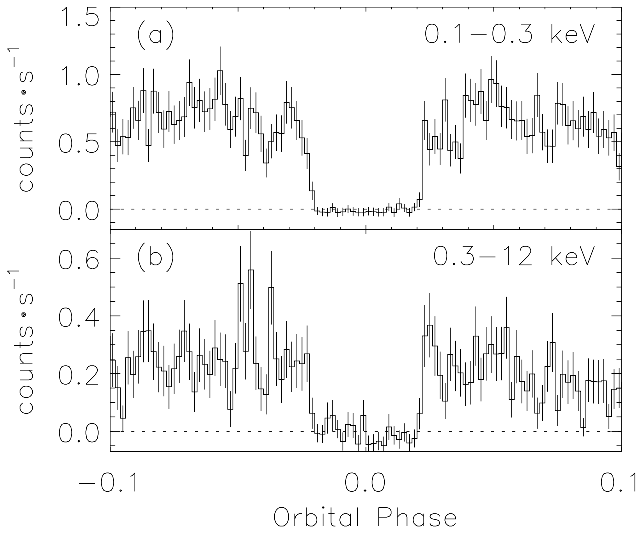

Figure 3. X-ray light curves for DP Leo around the eclipse with a bin size of 0.002 (10.8 s). *(a)* Blackbody component. *(b)* Bremsstrahlung component.

measurements can be used to determine the size and height of the emitting regions. The width of the bright phase was measured between the two points where the flux is halfway between its high and its low level. The centre of the bright phase at 0.002(2) corresponds to an accretion longitude of −1° ± 1°.

Fig. 4d shows the folded B-band light curve obtained with the *XMM-Newton* Optical Monitor. The higher flux level seen during the bright phase is most likely due to thermal emission from the heated photosphere near the accretion region. We measured a B magnitude of 20.2 during the faint phase and 19.6 at the peak. The centre of the bright phase at 0.01(1) coincides with that in the X-ray bands.

The R-band light curve in Fig. 4e was measured 32 hours before the *XMM-Newton* observation. It shows the double-peaked profile typical for cyclotron radiation from the accretion region. Since cyclotron radiation is preferentially emitted perpendicular to the magnetic field lines, the flux is highest near phase ±0.25 when the accretion region is seen edge-on and drops to nearly zero around the eclipse when the region is seen face-on. The fast rise and decline near phase ±0.3 is due to partial obscuration of the accretion region by the white dwarf. We determined the duration of this rise and decline and the width of the bright phase using the same method as for the X-ray light curves. Results are shown in Table 3. Since the companion star is not detected during the eclipse, the constant flux level in Fig. 4e seen during the faint phase is mainly due to thermal emission from the white dwarf. The contribution from the accretion stream or the heated side of the secondary is small since no significant modulation is seen between phases 0.3 and 0.7. We determined an R magnitude of 19.7 during the faint phase and 18.8 at the peaks.

Fig. 5 shows eclipse profiles in two X-ray bands and the B band. For the ingress and egress durations we find in the 2–12 keV band an upper limit of 30 s and in the 0.1–0.7 keV band a marginally non-zero value of 50 ± 40 s. The latter result is rather large compared to the upper limit of 7 s determined by Bailey et al. (1988) from optical observations. Our non-zero value may not be significant and rather due to the strong fluctuations and low statistics. In the B band we find non-zero ingress and egress durations of ∼40±20 s. This is expected since about half of the B-band emission originates from the photosphere away from the accretion spot and it roughly takes this long for the entire white dwarf to be eclipsed (Bailey et al. 1988).

Table 2. Overview of the parameters we derived for DP Leo. Values without explicit units are given in terms of orbital phase. Numbers in parentheses following the values are the uncertainties of the last digits at a 1-sigma level.

Eclipse centre (BJD in TT)	2451870.77690(4)
Eclipse period (P_{ecl})	0.062362821(2) d
Orbital conjunction (BJD in TT)	2451870.77682(4)
Orbital period (P_{orb})	0.062362820(2) d
Period change ($\dot{P}_{orb}$)	$-5.1(6) \cdot 10^{-12}$ s s^{-1}
Spin preriod (P_{spin})	0.062362766(5) d
Mass of secondary (M_2)	0.14(2) M$_\odot$
Mass ratio (q)	0.09–0.16
Orbital inclination (i)	81° ± 1°
Accretion longitude	25° ± 1°
Accretion longitude drift	2.3° ± 0.2° per year
Bright phase duration (0.3–12 keV)	0.57(1)
Bright phase centre (0.3–12 keV)	−0.070(3)
Eclipse width (0.1-12 keV)	0.0437(6) (235 ± 3 s)

2.5 Oscillations

The shock front in magnetic CVs may not be stable and oscillate on a time scale of seconds. In systems with a strong magnetic field, cyclotron cooling tends to suppress these quasi-periodic oscillations (QPOs) (Chanmugam et al. 1985). QPOs have been detected in the optical (Larsson 1989) but not as yet in X-rays. To search for oscillations we extracted X-ray light curves (0.1–12keV) with 0.01 s time bins and performed Discrete Fourier Transforms. We excluded the aforementioned time intervals of high background in the DP Leo observation and did not perform a background subtraction. No evidence for periodic or quasi-periodic oscillations was found in either source. For a strictly periodic signal we determined an upper limit of ∼10% for WW Hor and ∼22% for DP Leo over the frequency interval 0.1–10 Hz. It is more difficult to give accurate upper limits for QPOs, but we expect them to be comparable. For V834 Cen Imamura et al. (2000) found with *RXTE* data a similar upper limit of ∼14% at 90% confidence level for QPOs over the frequency range 0.2–1.2 Hz. Our limits are not strong enough to test shock oscillation models (Saxton & Wu 1999; Fischer & Beuermann 2001).

3 DISCUSSION

3.1 DP Leo

3.1.1 Accretion state

The X-ray peak flux we observed with *XMM-Newton* corresponds to a *ROSAT* PSPC count rate of roughly 1 photon per second. During a series of *ROSAT* observations in 1992

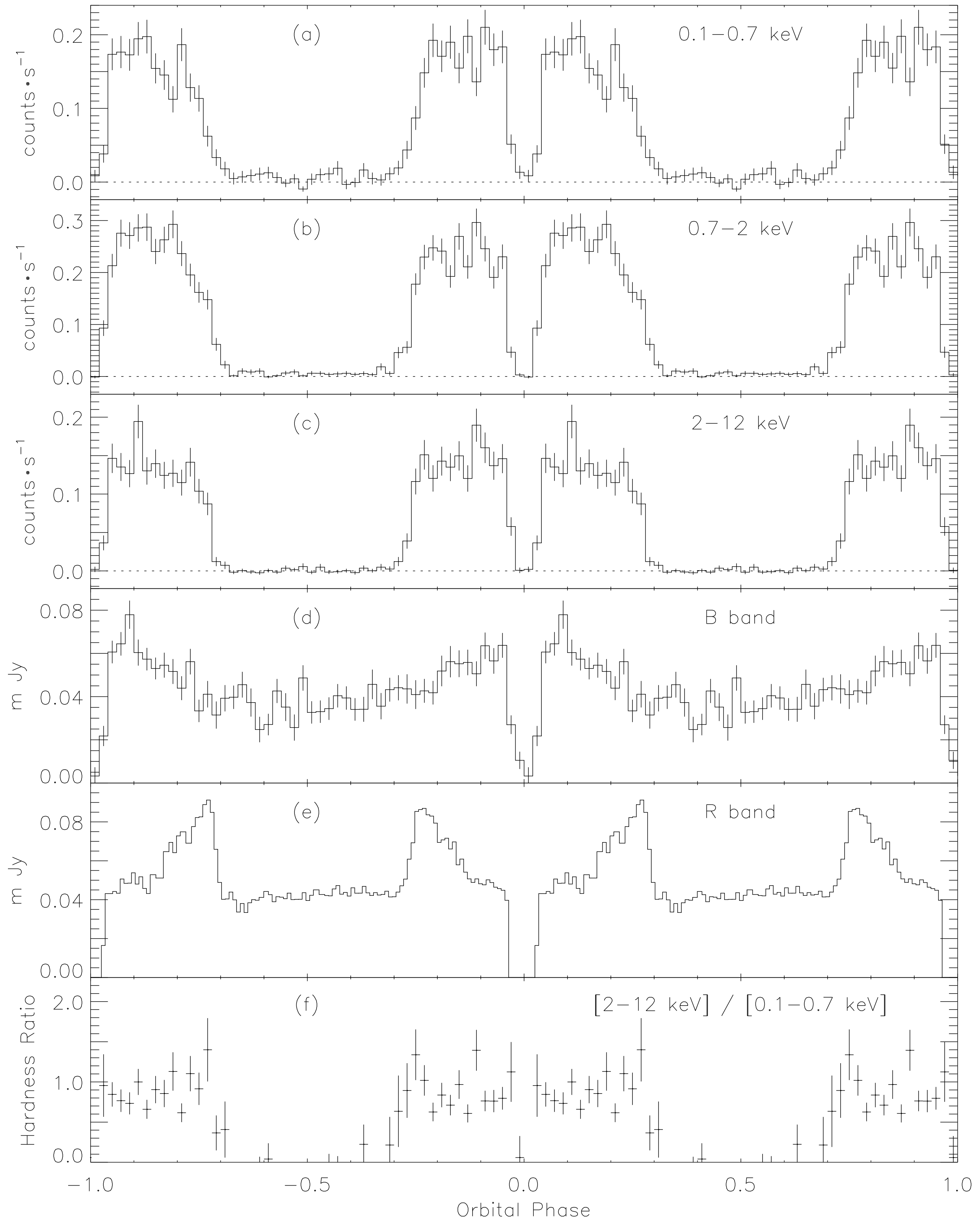

Figure 4. X-ray and optical light curves for WW Hor folded on the orbital period of 6929 s (115.5 min). *(a–c)* Folded X-ray light curves obtained with *XMM-Newton*. *(d)* Folded B-band light curve obtained with the *XMM-Newton* Optical Monitor. *(e)* R-band light curve obtained with the SAAO 1.0-m telescope. *(f)* Hardness ratio; Points with large uncertainties have been omitted.

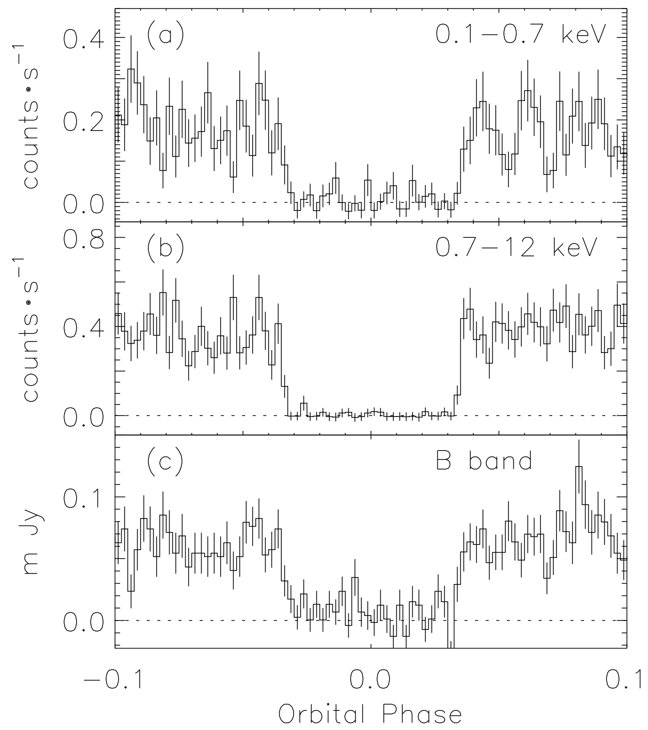

Figure 5. X-ray and optical light curves for WW Hor around the eclipse with a bin size of 0.0025 (17.3 s).

Table 3. Overview of the parameters we derived for WW Hor. Values without explicit units are given in terms of orbital phase. Numbers in parentheses following the values are the uncertainties of the last digits at a 1-sigma level.

Eclipse centre (BJD in TT)	2451882.73354(5)
Eclipse period	0.0801990403(9) d
Mass of secondary (M_2)	0.19(2) $M_\odot$
Mass ratio (q)	0.14–0.22
Orbital inclination (i)	84° ± 2°
Accretion colatitude (δ)	64° − 104°
Accretion longitude	−1° ± 1°
Optical magnitudes	
B band (peak/faint phase)	19.6 / 20.2
R band (peak/faint phase)	18.8 / 19.7
Bright phase width	
X-rays (0.1–0.7 keV)	0.515(7)
X-rays (2–12 keV)	0.530(4)
R band	0.551(4)
Bright phase centre	
X-rays (0.1–12 keV)	0.002(2)
B band	0.01(1)
Bright phase rise/decline width	
X-rays (0.1–0.7 keV)	0.09(2) / 0.12(2)
X-rays (2–12 keV)	0.06(1) / 0.06(1)
R band	0.04(1) / 0.03(1)
Width of eclipse	
X-rays (0.1–12 keV)	0.0682(7) (473 ± 5 s)
B band	0.068(2) (470 ± 14 s)

DP Leo was found in a similar state of accretion with a peak flux varying between 0.5 and 2 photons per second (Robinson & Cordova 1994). Three months earlier an optical peak magnitude of R=17.9 was measured (Bailey et al. 1993). From CCD images taken with the JKT 1.0-m telescope on La Palma (J. Etherton, priv. comm.) one day after the *XMM-Newton* observation we obtain a similar magnitude of R∼17.5-17.6 (at phase 0.13 near the suspected peak). This is one magnitude fainter than the R=16.5 measured during the high state in 1982 (Biermann et al. 1985). A lower state with a peak magnitude R∼18.2 has also been observed (Stockman et al. 1994). We conclude that during the *XMM-Newton* observation DP Leo was in an intermediate state of accretion.

3.1.2 Orbital parameters

For cataclysmic variables the mass of the Roche-lobe filling secondary can be inferred from the orbital period, given the mass-radius relationship of the star. From mass-period relationships derived empirically (Warner 1995; Smith & Dhillon 1998) and with evolutionary models (Howell et al. 2001) we estimate for DP Leo a secondary mass $M_2 = 0.14 \pm 0.02\ M_\odot$. Here the assumption was made that DP Leo has not yet evolved past the 80-min period minimum. In Ramsay et al. (2001) we derived a white dwarf mass $M_1 \sim 1.4\ M_\odot$. This is rather high and might be an overestimate. With the conservative assumption $M_1 \approx 1.0$–$1.4\ M_\odot$ we obtain a mass ratio $q \approx 0.09$–0.16. For eclipsing CVs the orbital inclination can be derived from the duration of the eclipse and the mass ratio (Chanan et al. 1976). With the eclipse duration of 235 s we obtain an inclination $i = 81^\circ \pm 1^\circ$. This is consistent with the result $i = 76^\circ \pm 10^\circ$ by Biermann et al. (1985). The accretion colatitude δ can in principle be derived from the duration of the bright phase $\Delta\Phi$ using equation (1) in Section 3.2.5. However, since the accretion spot is most likely not small, the measured bright phase duration is longer than the $\Delta\Phi_0$ needed in equation (1). It is possible to correct for this difference, but because of the uncertain accretion spot size we were not able to obtain useful constraints for the colatitude. The best available measurement from previous observations is $\delta = 103^\circ \pm 5^\circ$ (Biermann et al. 1985).

3.1.3 Eclipse ephemeris and orbital period change

In Fig. 6a we compare our measurement of the time at which the eclipse occurred with previous results by Robinson & Cordova (1994); Stockman et al. (1994); Schmidt (1988); Biermann et al. (1985). To account for leap seconds accumulated over the past 20 years we converted the eclipse timings from these papers, originally in HJD (UTC), to BJD (TT). Fig. 6a shows the deviation of the measured time of eclipse from a linear ephemeris (dashed line) that was obtained by fitting only the data points between 1979 and 1993. During the *XMM-Newton* observation in November 2000 the eclipse occurred ∼70 s earlier than predicted by the linear ephemeris. This is clear evidence that the orbital period P_{orb} of the system has been decreasing over the past 20 years. Marginal evidence for a changing P_{orb} was found by Stockman et al. (1994).

The solid curve in Fig. 6a shows the result of a quadratic fit to all data points including our measurement. From this fit we obtain an improved eclipse ephemeris that now con-

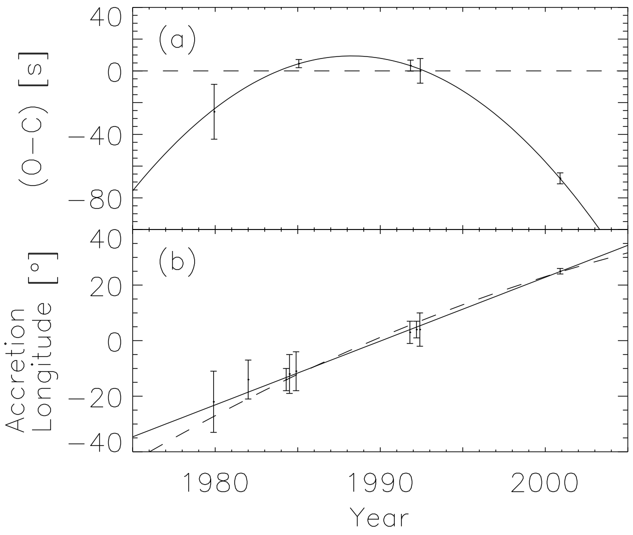

Figure 6. DP Leo: *(a)* Deviation of the time when the eclipse occurred from a linear ephemeris (dashed line) that was obtained by fitting only the data points between 1979 and 1993. The solid curve is the best fit of a quadratic ephemeris to all data points. *(b)* Accretion longitudes measured over the past 20 years. The solid line is a linear fit with a slope of 2.3° ± 0.2° per year. The dashed curve shows a fit corrected for the change in orbital period.

tains a quadratic term to account for the non-zero $\dot{P}_{orb}$:

$$\begin{aligned} \text{BJD (TT)} \quad 2451870.77690(4) \quad &+ \quad 0.062362821(2) \cdot E \\ &- \quad 1.6(2) \cdot 10^{-13} \cdot E^2 \end{aligned}$$

The quadratic term corresponds to an orbital period change $\dot{P}_{orb} = -5.1(6) \cdot 10^{-12}$ s s^{-1}, which gives a characteristic time scale $P_{orb}/\dot{P}_{orb} = -3.3(4) \cdot 10^7$ yrs. This is one order of magnitude shorter than the time scale of $-5 \cdot 10^8$ yrs expected for angular momentum loss by gravitational radiation alone (Wickramasinghe & Wu 1994).

The eclipse ephemeris slightly differs from the ephemeris for orbital conjunction because the accretion region is 25° ahead of the secondary. Using the result by Stockman et al. (1994) that it takes 51 s to eclipse the entire white dwarf and with the orbital parameters in Table 2, we estimate that during the *XMM-Newton* observation orbital conjunction occurred 8 s before the centre of the eclipse was seen. By applying similar corrections to all previous measurments we obtain an ephemeris for orbital conjunction:

$$\begin{aligned} \text{BJD (TT)} \quad 2451870.77682(4) \quad &+ \quad 0.062362820(2) \cdot E \\ &- \quad 1.6(2) \cdot 10^{-13} \cdot E^2 \end{aligned}$$

3.1.4 Accretion longitude changes

The simple and symmetric shape of the hard X-ray light curves (Fig. 2b,c) allowed us to determine the accretion longitude with high accuracy (25° ± 1°). In Fig. 6b we compare our result with earlier measurements by Robinson & Cordova (1994); Stockman et al. (1994); Bailey et al. (1993); Biermann et al. (1985). The data suggest that the accretion longitude has been increasing linearly with time over the past 20 years. From a linear fit we find a longitude drift of 2.3° ± 0.2° per year (solid line in Fig. 6b). This drift is likely caused by a slightly asynchronous rotation of the white dwarf. If the accretion spot is fixed relative to the magnetic poles, then the spin period of the white dwarf must be 5.9(5) ms shorter than the orbital period. This corresponds to a relative deviation of $1.1(1) \times 10^{-6}$ s s^{-1} and a synodic period of ∼160 years. The actual deviation between the two periods might be somewhat different, since changes in the orientation of the magnetic axis are likely to affect the location of the accretion spot.

Magnetic interactions between the two stars are expected to spin down the white dwarf toward synchronism on a time-scale of ∼200 years (Campbell & Schwope 1999). However, for DP Leo the orbital period is decreasing faster than the spin period is increasing so that synchronism will be achieved on a shorter time-scale. The dashed curve in Fig. 6b shows a fit to the accretion longitudes taking into account the change in orbital period. Here we assumed that the spin period P_{spin} and the orbital period change $\dot{P}_{orb}$ are constant. We find that in December 2000 the spin period was 8.6×10^{-7} s s^{-1} shorter than the orbital period and that DP Leo will achieve synchronism in the year 2030. However, the white dwarf spin will not remain sychronized as the orbital period continues to decrease, leading to an under-synchronous rotation and a decreasing spot longitude.

3.1.5 Hard X-ray light curves

The X-ray light curves of the bremsstrahlung component (Fig. 2b,c) closely follow a cosine profile during the bright phase. This is an unexpected result, since the region emitting the bremsstrahlung is thought to be optically thin and the light curves should have a top-hat shape. A similar cosine profile was seen before with *ROSAT* and *Einstein* (Robinson & Cordova 1994). However, these observatories most likely did not detect the bremsstrahlung component but rather the dominating soft blackbody component: this emission originates from the optically thick photosphere and is expected to produce a cosine-shaped light curve.

Imamura & Durisen (1983) calculated X-ray light curves for the bremsstrahlung component in polars. They showed that for a system with orbital inclination $i \approx 90°$ the light curve has a top-hat shape if the accretion region is near the equator, but can also have a shape closer to a cosine if accretion occurs near the rotational poles. In the latter case the post-shock region is always viewed from the side and, since it is much more horizontally than vertically extended, might always appear optically thick. However, the accretion rate in DP Leo was $\sim 10^2$ times lower than the rates assumed by the authors, so that the optical depth might be significantly less.

Unfortunately we are unable to constrain the colatitude of the accretion region (Section 3.1.2). If accretion does occur close to the lower rotational pole ($\delta \approx 180°$), then the model by Imamura & Durisen (1983) might be able to explain the observed cosine profile. However, it is not clear why the accretion region would have migrated this far from its 1984 location at $\delta \approx 100°$ (Biermann et al. 1985). The considerable shift in accretion longitude by ∼40° since 1984 suggests that significant changes in the entire accretion geometry have occurred. However, a shift in colatitude would have caused a change in the bright phase duration which is not observed. If the accretion spot is still near the equator as in 1984, then optical depth effects as discussed in Cropper et al. (2000) are also important when the accretion region is seen face-on.

The observed hard X-ray light curve cannot be easily explained by an optically thin, but horizontally extended emission region. Since the flux is at its highest level for only a short period ($\leq$0.2 in phase), an optically thin region would have to be partially obscured during most of the bright phase. For this to be possible an accretion region near the equator would have to be almost as large as the white dwarf. The accretion region in DP Leo is much smaller than this, only $\sim$15% of the white dwarf diameter (Bailey et al. 1993). An optically thin region of this size can only produce the observed light curve if it is located at high colatitudes ($\delta \approx 170^\circ$). As discussed in the previous paragraph, the accretion region in DP Leo is more likely close to $\delta \approx 100^\circ$.

Optical depth effects in the accretion column are likely to affect the X-ray spectrum (e.g. Hellier et al. 1998). However, current models do not consider optically thick post-shock regions and it is difficult to predict how the spectrum will deviate from the optically thin case. One might expect to see a blackbody-like spectrum that is modified somewhat due to the inhomogeneous temperature and density distribution and that changes with the viewing angle. Yet for DP Leo the X-ray spectrum above 0.3 keV is well fit by an optically thin bremsstrahlung model (Ramsay et al. 2001) and the spectral slope apparently does not vary during the bright phase (Fig. 2b,c). It is generally thought that free-free absorption is negligible for X-rays in the post-shock region. However, the optical depth due to electron scattering might be significant (Cropper et al. 2000; Rosen 1992). In a post-shock region with an optical depth for electron scattering larger than unity and with negligible free-free absorption, the photons produced by bremsstrahlung are typically not reabsorbed, but are scattered until they escape from the region. Electron scattering is wavelength independent and, if the photon energies are not significantly changed by the thermal motion of the electrons, the energy distribution of the escaping photons should be very similar to their original bremsstrahlung spectrum. Because the region is optically thick for electron scattering, the observed flux depends mainly on the projected area and should vary like a cosine, just as it does for DP Leo. So if electron scattering is the major source of opacity, it is possible to obtain the spectrum of optically thin bremsstrahlung even if the post-shock region is optically thick. Of course, for a more realistic picture other effects like cyclotron cooling, inverse compton scattering and the accretion column structure need to be considered.

3.1.6 Soft X-ray light curve

The soft X-ray light curve (Fig. 2a) has a complex and asymmetric shape very different from the simple cosine profile seen in the hard X-ray bands (Fig. 2b,c). Strong asymmetries in the X-ray and optical light curves of DP Leo have been observed before (Robinson & Cordova 1994; Bailey et al. 1993). The hardness ratio in Fig. 2e shows a softening of the spectrum throughout the bright phase. These variations might be due to photoelectric absorption of the soft X-rays by an asymmetric accretion curtain. A column density $N_H \sim 10^{20}\mathrm{cm}^{-2}$ is required to explain the amplitude of the observed changes.

As an alternative explanation we suggest that the structure in the soft X-ray light curve might be caused by additional accretion regions only visible at energies below 0.3 keV. Almost all of the emission in the 0.1–0.3 keV band is blackbody radiation from the photosphere below the shock (Ramsay et al. 2001). Since the main accretion region is small ($\sim$0.15 R_{WD}; e.g. Bailey et al. 1993) and near the equator, the soft X-ray light curve in Fig. 2a should be cosine-shaped similar to the light curves in Fig. 2b,c. Such a cosine profile for the soft X-ray emission was seen before with *ROSAT* and *Einstein* (Robinson & Cordova 1994). Fig. 1a shows that some of the deviation from the expected cosine profile is due to short flares. Yet the asymmetry seen in Fig. 2a is present for all three orbital cycles and it appears that the flares are concentrated around the eclipse. If only one accretion region is present, we would expect to see a symmetric light curve and the flares should be more evenly spread over the bright phase. However, the soft X-ray light curve could be explained with a second accretion region that is at higher colatitudes than the main region and has a shorter bright phase. Unfortunately the *XMM-Newton* observation covered only three orbital cylces and it is difficult to know how permanent the features in Fig. 2a are.

If the structure in the soft X-ray light curve is indeed caused by additional accretion regions, it is possible to derive their location on the white dwarf. The soft X-ray emission from the main accretion region is expected to produce a cosine-shaped light curve with the same bright phase duration of 0.57 that was found in the 0.3–12 keV band. We therefore subracted this cosine profile from the soft X-ray light curve (Fig. 2a), which would ideally remove the contribution from the main region. The normalization was chosen such that the residual is as small as possible but not negative beyond statistical fluctuations. The residual light curve (Fig. 2d) shows a broad peak centred around the eclipse and a narrower peak centred at phase 0.17. These peaks could be interpreted as emission from two regions near the lower rotational pole. By measuring the peak width and centre we can determine the locations of the associated regions with equation (1) in Section 3.2.5. We find for the larger peak a longitude of -2° and a colatitude of $> 164^\circ$ and for the smaller peak a longitude of -61° and a colatitude of $\sim 172^\circ$. In comparison the main accretion region was found at 25° longitude and the colatitude was not constrained (Sections 2.3 and 3.1.2).

If these additional emission regions exist, it should be possible to distinguish them in the eclipse profile from the main accretion region. With the orbital parameters in Table 2 we find that during ingress the limb of the secondary moves across the white dwarf at an angle of about $+45^\circ$ with respect to the rotational axis while during egress it does so at an angle of -45°. With a colatitude $\delta = 103^\circ$ for the main region (Biermann et al. 1985) and using the result by Stockman et al. (1994) that it takes 51 s for the secondary to eclipse the entire white dwarf, we estimate that during ingress the second region would be eclipsed 20 s earlier than the main region, but during egress it would be eclipsed 4 s later. This is in agreement with the eclipse profile in Fig. 3a, which shows a significantly longer ingress than egress duration. In the figure a time difference of 20 s corresponds to roughly 2 bins. However, we cannot exclude the possibility that the longer ingress duration was caused by statistical fluctuations or flaring. The model of a second emission region near the rotational pole and in longitude behind the main region could also account for the asymmetries seen in the X-ray and optical light curves from previous observations (Robinson & Cordova 1994; Bailey et al. 1993).

3.2 WW Hor

3.2.1 *Accretion state*

During the *XMM-Newton* observation of WW Hor we measured optical peak magnitudes of $B = 19.6$ and $R = 18.8$. Similar values of $B = 19.6$ and $R = 18.3$ were found in a 1992 observation (Bailey et al. 1993). One week earlier the *ROSAT* PSPC measured a peak flux of 0.08 photons per second (Tennant et al. 1994). This is comparable to the *XMM-Newton* flux which corresponds to a *ROSAT* PSPC count rate of ∼0.06 photons per second. WW Hor was apparently in similar accretion states during the *XMM-Newton* and the 1992 observation. In 1987 WW Hor was found in a higher state with magnitudes of $B = 18.6$ and $R = 17.1$ (Bailey et al. 1988). Accretion states lower than in December 2000 have not been observed, but since strong cyclotron emission is visible in our R-band data (Fig. 4e) we conclude that WW Hor was in an intermediate state of accretion.

3.2.2 *Orbital parameters*

The orbital parameters of WW Hor can be derived in a similar way as shown in Section 3.1.2. From the 115.5-min orbital period we find a secondary mass $M_2 = 0.19 \pm 0.02$ M$_\odot$ and with the white dwarf mass $M_1 \approx 0.9$–1.3 M$_\odot$ (Ramsay et al. 2001) a mass ratio $q \approx 0.14$–0.22. By combining this with the eclipse duration of 473 s we obtain an orbital inclination $i = 84^\circ \pm 2^\circ$. The accretion colatitude δ can be derived from the bright phase duration $\Delta\Phi$ using equation (1) in Section 3.2.5. By measuring $\Delta\Phi$ between the points where the flux is halfway between its high and its low level, the complications from the uncertain accretion spot size we encountered for DP Leo can be avoided. As shown in Table 3, the bright phase widths differ between energy bands, which is probably due to different heights above the surface. If we assume that $\Delta\Phi_0 = 0.515$, i.e. the 0.1–0.7 keV flux originates from a region at zero height, we find an accretion spot colatitude $\delta \approx 66^\circ \pm 13^\circ$. Since this assumption might not be valid, we use the R-band light curve (Fig. 4e) to obtain a more reliable constraint for δ. The flux from cyclotron emission around the eclipse is less than ∼10% of its peak value. From the $\sin^2\alpha$ dependence of the flux we therefore know that around the eclipse the angle α between the line of sight and the magnetic field lines is less than 20°. If the magnetic field is perpendicular to the surface, this requires that δ and i differ by at most 20°, i.e. $\delta \approx 64^\circ - 104^\circ$.

3.2.3 *Eclipse ephemeris*

The eclipse observed with *XMM-Newton* occurred as predicted by the latest ephemeris (Beuermann et al. 1990) which had an accumulated uncertainty of ∼40 s. We obtain an updated ephemeris by converting the mid-eclipse times in table 2 of Beuermann et al. (1990) from HJD (UTC) to BJD (TT) and combining them with our measurement:

$$\text{BJD (TT)}\ \ 2451882.73353(5) + 0.0801990403(9) \cdot E$$

Since no change in orbital period is seen, we can place an upper limit of $5 \cdot 10^{-12}$ s s^{-1} on $\dot{P}_{orb}$ or a lower limit of $4 \cdot 10^7$ yrs on $P_{orb}/\dot{P}_{orb}$.

Table 4. Horizontal and vertical extent of the emission region in WW Hor (see Section 3.2.5). *2nd column* is the horizontal extent in a longitudinal direction. *3rd–5th column* is the height in units of white dwarf radius for three assumed colatitudes δ inside the allowed range $64^\circ - 104^\circ$ from Section 3.2.2.

Energy band	Extent in longitude	Height in units of R_{WD} $\delta = 64^\circ$	$\delta = 84^\circ$	$\delta = 104^\circ$
0.1-0.7 keV	$38^\circ \pm 6^\circ$	0.000	0.001	0.002
2-12 keV	$22^\circ \pm 4^\circ$	0.001	0.003	0.007
R band	$13^\circ \pm 4^\circ$	0.005	0.011	0.016

3.2.4 *Accretion longitude changes*

From the X-ray light curves we derived an accretion longitude of $-1^\circ \pm 1^\circ$. Bailey et al. (1993) determined a similar value of $-3.6^\circ \pm 2.5^\circ$ in 1992, when WW Hor was in a similar intermediate state of accretion. The authors found a significantly different value of $11.2^\circ \pm 1.8^\circ$ for 1987, when WW Hor was in a high accretion state and brighter by 1.7 magnitudes in R. These data are not consistent with a linear time dependence of the longitude, but rather suggest a correlation with the accretion rate. The observed longitude variations might be due to a changing location of the accretion spot on the white dwarf's surface, while the orientation of the magnetic axis relative to the secondary remains fixed.

3.2.5 *Accretion region geometry*

As discussed in Ramsay et al. (2001), the X-ray spectrum of WW Hor does not appear to contain the soft blackbody component usually seen in polars. The light curves shown in Fig. 4a–c therefore represent different energy ranges of the bremsstrahlung component. Their top-hat like shape is as expected for the optically thin bremsstrahlung emission and in agreement with models of the post-shock region (Cropper et al. 2000; Imamura & Durisen 1983). By measuring the shape of the X-ray and R-band light curves we are able to constrain the horizontal and vertical extent of the emission region.

In the idealized case of an optically thin and point-like emission region at zero height the light curve is expected to have a perfect top-hat shape and the duration of the bright phase $\Delta\Phi_0$ is given by

$$\cot i \cdot \cot \delta = -\cos(180^\circ \cdot \Delta\Phi_0) \qquad (1)$$

Here i is the orbital inclination, δ is the colatitude of the emission region and $\Delta\Phi_0$ has units of orbital phase. If the emitting region is not point-like but extended horizontally, the transition between bright and faint phases is more gradual than for a top-hat profile. The duration of this transition is equal to the time it takes the accretion region to move over the horizon of the white dwarf and therefore is a direct measure for the angular size of the region in a longitudinal direction. The angular size does not depend on the width of the bright phase which is a measure for the height of the region (see next paragraph). Table 4 (2nd column) shows the angular sizes we obtain by converting the rise and decline widths from Table 3 into degrees. We find that the soft X-ray emitting region with a size of ∼40° is about twice as large as the region in which the hard X-rays are produced. This suggests that the temperature in the post-shock region is not uniform across the spot but rather increases toward the centre. The emission in the R-band originates from an even smaller region, indicating that efficient production of cyclotron radiation requires even higher temperatures than the emission of hard X-rays via bremsstrahlung.

For an extended emission region equation (1) is still valid if the width of the bright phase $\Delta\Phi_0$ is measured between the two points where the flux is halfway between its high and its low level. However, for a region with a significant height above the surface the measured width $\Delta\Phi$ is longer than the $\Delta\Phi_0$ predicted by equation (1). Given the inclination i and colatitude δ we can calculate $\Delta\Phi_0$ with equation (1) and then estimate the height H from the measured width $\Delta\Phi$ using the relation

$$H = \frac{1}{2}\,\pi^2 \cdot (\Delta\Phi - \Delta\Phi_0)^2 \cdot \sin^2 i \cdot \sin^2\delta \cdot R_{WD} \qquad (2)$$

which is valid for $H \ll R_{WD}$. Here $\Delta\Phi$ and $\Delta\Phi_0$ have units of orbital phase and R_{WD} is the radius of the white dwarf. Table 4 shows the values of H we obtain from the bright phase widths in Table 3 for three assumed colatitudes δ inside the allowed range from Section 3.2.2. The cyclotron radiation originates from a height of $\sim 0.01\ R_{WD}$ while the bremsstrahlung component is produced much closer to the surface. We also find that the soft X-rays are emitted at a lower height than the hard X-rays. This result is consistent with the picture that the gas in the post-shock region is hottest just below the shock front and then cools and compresses as it falls toward the surface (Cropper et al. 2000). The energy output from cyclotron radiation has a stronger temperature dependence than that from bremsstrahlung, so we expect to see the optical cyclotron emission from higher up in the post-shock region where the gas is hotter. Also the power radiated via bremsstrahlung depends quadratically on the density while that for cyclotron radiation does so only linearly. Therefore bremsstrahlung is preferably emitted from a lower height where the gas is more compressed. Because of the lower temperatures and higher densities at the bottom of the post-shock region it is also expected that the soft X-rays are produced at a lower height than the hard X-rays.

The above method to disentangle size and height is fairly accurate if the thickness of the emission region is small compared to its height. Even if this is not the case, equation (2) still yields a good estimate for the average height. However, the size of a homogeneous emission region extending from height H_1 to H_2 will be overestimated by an angle $\sim 400^\circ \cdot (\sqrt{H_2} - \sqrt{H_1}) \cdot \sin^2 i \cdot \sin^2\delta$. For instance a thickness of 0.005 R_{WD} and a height of 0.01 R_{WD} will lead to a deviation of ∼10°. Another systematic error might be introduced into the height determination, if the emission region becomes optically thick when viewed edge-on. In this case the width of the bright phase is smaller than expected and the height would be underestimated. Further studies of the light curve profiles should certainly include 3-dimensional modeling of the temperature and density distributions in the post-shock region and take into account optical depth effects (Cropper et al. 2000; Imamura & Durisen 1983).

From observations done in 1987, Bailey et al. (1988) found a bright phase width for the cyclotron component of $\Delta\Phi = 0.585$. This is significantly larger than our measurement of $\Delta\Phi = 0.551$. We could attribute this discrepancy to a change in the height of the shock. With the 1987 value for $\Delta\Phi$ we find a height of ∼0.019–0.040 which is about 3 times larger than during the *XMM-Newton* observation. This is surprising since in 1987 the total accretion rate was higher (see Section 3.2.1) and according to current models the shock should have been lower. It is possible that in 1987 the accretion spot was significantly larger so that the accretion rate per area was actually lower than during the *XMM-Newton* observation, which would lead to a larger height of the shock. The difference between the two observations might also be due to a change in the colatitude of the accretion region. However, this is less likely since the orbital inclination near 90° would require a very large colatitude change.

4 CONCLUSIONS

We have performed extensive *XMM-Newton* observations of two magnetic cataclysmic variable stars, DP Leo and WW Hor. From a comparison with previous observations we conclude that both objects were in an intermediate state of accretion. We derived for both systems the mass ratio, orbital inclination and an improved eclipse ephemeris. We examined the X-ray data for periodic and quasi-periodic oscillations, but found no evidence for them in either source.

4.1 DP Leo

From the shape of the hard X-ray light curves we conclude that the post-shock region has a significant optical depth. Although the X-ray spectrum indicates optically thin bremsstrahlung, it might still be consistent with an optically thick post-shock region if electron scattering is the major source of opacity. We find a strong asymmetry in the shape of the soft X-ray light curve which is not seen for the hard X-rays. This asymmetry can be explained with photoelectric absorption by the accretion curtain ($N_H \sim 10^{20}\mathrm{cm}^{-2}$) or with two additional accretion regions near the lower rotational pole. By comparing our measurement of the accretion spot longitude with previous results, we find that the longitude is changing linearly in time by 2.3° per year. This is likely due to the rotational period of the white dwarf being shorter than the orbital period by $\sim 1\times10^{-6}$ s s^{-1}. From a comparison with previous results we find that our measurement of the time of eclipse is not consistent with a linear ephemeris and that instead the orbital period of the system is decreasing on a time scale $P_{orb}/\dot{P}_{orb} = -3.3\cdot10^7$ yrs. This change is one order of magnitude faster than expected for energy loss by gravitational radiation alone.

4.2 WW Hor

We use the shape of the X-ray light curves to derive the horizontal and vertical extent of the post-shock region. We find that the soft X-rays originate from a region that has a longitudinal extent of ∼40° while the hard X-rays are emitted in a region about half this size. This result shows that the temperature of the post-shock gas is increasing toward the centre. We find that the cyclotron radiation originates from a height of ∼1% of the white dwarf radius while the X-rays are emitted at a much lower height. This is consistent with the general prediction that the temperature decreases and the density increases as the gas settles onto the surface. By comparing our measurement with previous results we find that the accretion longitude is correlated with the accretion rate. This indicates that the observed longitude variations are due to a changing location of the accretion spot and not a change in the relative orientation of the magnetic axis.

ACKNOWLEDGEMENTS

This work is based on observations obtained with *XMM-Newton*, an ESA science mission with instruments and contributions directly funded by ESA Member States and the USA (NASA). D.P. acknowledges support from NASA grant NAG5-7714. We thank Jason Etherton for the optical data of DP Leo he obtained with the JKT (La Palma).

REFERENCES

Bailey J., Wickramasinghe D. T., Ferrario L., Hough J. H., Cropper M., 1993, MNRAS, 261, L31
Bailey J., Wickramasinghe D. T., Hough J. H., Cropper M., 1988, MNRAS, 234, 19P
Beuermann K., Thomas H. ., Schwope A. D., Giommi P., Tagliaferri G., 1990, A&A, 238, 187
Beuermann K., Thomas H. C., Giommi P., Tagliaferri G., 1987, A&A, 175, L9
Biermann P., Schmidt G. D., Liebert J., Tapia S., Strittmatter P. A., West S., Stockman H. S., Kuehr H., Lamb D. Q., 1985, ApJ, 293, 303
Campbell C. G., Schwope A. D., 1999, A&A, 343, 132
Chanan G. A., Middleditch J., Nelson J. E., 1976, ApJ, 208, 512
Chanmugam G., Langer S. H., Shaviv G., 1985, ApJ, 299, L87
Cropper M., 1990, Space Science Reviews, 54, 195
Cropper M., Wu K., Ramsay G., 2000, New Astronomy Review, 44, 57
Fischer A., Beuermann K., 2001, A&A, 373, 211
Hellier C., Mukai K., Osborne J. P., 1998, MNRAS, 297, 526
Howell S. B., Nelson L. A., Rappaport S., 2001, ApJ, 550, 897
Imamura J. N., Durisen R. H., 1983, ApJ, 268, 291
Imamura J. N., Steiman-Cameron T. Y., Wolff M. T., 2000, PASP, 112, 18
Kuijpers J., Pringle J. E., 1982, A&A, 114, L4
Larsson S., 1989, A&A, 217, 146
Mason K. O., Breeveld A., Much R., Carter M., Cordova F. A., Cropper M. S., Fordham J., Huckle H., Ho C., Kawakami H., Kennea J., Kennedy T., Mittaz J., Pandel D., Priedhorsky W. C., Sasseen T., Shirey R., Smith P., Vreux J. ., 2001, A&A, 365, L36
Ramsay G., Cropper M., Córdova F., Mason K., Much R., Pandel D., Shirey R., 2001, MNRAS, 326, L27
Robinson C. R., Cordova F. A., 1994, ApJ, 437, 436
Rosen S. R., 1992, MNRAS, 254, 493
Saxton C. J., Wu K., 1999, MNRAS, 310, 677
Schmidt G. D., 1988, The current observational outlook on AM Herculis variables. Polarized Radiation of Circumstellar Origin, p. 85
Schwope A. D., Hambaryan V., Schwarz R., 2002, A&A, in press (astro-ph 0111457)
Smith D. A., Dhillon V. S., 1998, MNRAS, 301, 767
Stockman H. S., Schmidt G. D., Liebert J., Holberg J. B., 1994, ApJ, 430, 323
Tennant A. F., Bailey J., Wickramasinghe D. T., Wu K., Ferrario L., Hough J., 1994, MNRAS, 271, 733
Warner B., 1995, Cataclysmic variable stars. Cambridge Astrophysics Series, Cambridge, New York: Cambridge University Press
Wickramasinghe D. T., Wu K., 1994, Ap&SS, 211, 61
Wu K., 2000, Space Science Reviews, 93, 611